

# Silver nanowires electrodeposited into nanoporous templates: Study of the influence of sizes on crystallinity and structural properties

E.A. Dalchiele<sup>a,\*</sup>, R.E. Marotti<sup>a</sup>, A. Cortes<sup>b</sup>, G. Riveros<sup>c</sup>, H. Gómez<sup>b</sup>, L. Martínez<sup>d</sup>,  
R. Romero<sup>d</sup>, D. Leinen<sup>d</sup>, F. Martín<sup>d</sup>, J.R. Ramos-Barrado<sup>d</sup>

<sup>a</sup>*Instituto de Física, Facultad de Ingeniería, Herrera y Reissig 565, C.C. 30, 11000 Montevideo, Uruguay*

<sup>b</sup>*Instituto de Química, Facultad de Ciencias, Universidad Católica de Valparaíso, Casilla 4059, Valparaíso, Chile*

<sup>c</sup>*Facultad de Ciencias, Universidad de Valparaíso, Avda. Gran Bretaña 1111, Playa Ancha, Valparaíso, Chile*

<sup>d</sup>*Laboratorio de Materiales y Superficie (Unidad Asociada al CSIC), Departamentos de Física Aplicada & Ingeniería Química, Universidad de Málaga, Málaga, Spain*

Available online 22 August 2006

## Abstract

In this work, results on the study of the influence of silver nanowire dimensions on the crystallinity and structural properties are presented. Silver nanowire arrays with high aspect ratios were prepared in the hollow structures of nanoporous templates using potentiostatic electrodeposition. Two types of material were employed as a template: commercial porous anodic aluminum oxide (with a mean pore diameter of 180 nm) and track-etched polycarbonate membranes (with a mean pore diameter of 15, 30 and 80 nm). Characterization of the silver nanowires has been done by EDS, XRD, TEM and electron diffraction. The degree of preferred crystallographic orientation (along the (1 1 1), (2 0 0) or (2 2 0) crystallographic planes) and the crystallite size of the silver nanowires as a function of template pore diameter are given and discussed.

© 2006 Elsevier B.V. All rights reserved.

PACS: 61.46.–w; 81.07.–b; 82.45.Aa

Keywords: Nanowires; Silver; Electrodeposition; Texture

## 1. Introduction

Metallic nanowires are of great interest both for nanotechnological applications and for nanoscience studies because of their extraordinary electronic, optical and chemical properties. Applications have been studied in the areas of plasmonics [1], nanoelectronics [2], nanobiotechnology [3], biology [4], superconductivity [5,6], magnetic sensors based on the giant magneto-resistance effect [7,8], ultra high-density magnetic recording media systems [9], low-voltage field emitter arrays [10], and thermoelectric devices [11]. Moreover, with the rapid decrease in the size of electronic devices, metallic nanowires can play an important role in the middle scale of 10–200 nm to connect

molecular scale devices to the macroscale world [12], and to connect different elements in nano-electronics.

In recent years, the electrodeposition into nanoporous membrane templates, pioneered by Possin [13] and Martin [14], has provided a versatile approach used by a number of researchers to prepare freestanding nanowires of metals, semiconductors, and polymers [15–17].

Silver nanowires are of special interest because, of all the metals, silver exhibits the highest electrical conductivity, and the silver nanowire surface can enhance the Raman scattering of molecules absorbed on its surface [18]. Furthermore, since the electrical, thermal and mechanical properties of nanowires are very dependant on their structural and morphological characteristics, the creation of high quality nanostructures with well-controlled crystallinity is a challenging task.

In this study, silver nanowire arrays were potentiostatically electrodeposited into alumina and track-etched

\*Corresponding author. Tel.: +598 2 7110905; fax: +598 2 7111630.  
E-mail address: [dalchiel@fing.edu.uy](mailto:dalchiel@fing.edu.uy) (E.A. Dalchiele).

polycarbonate (PC) membranes containing nanopores from 30 to 180 nm in diameter. The structural and crystallinity results are presented here.

## 2. Experimental details

The details for the electrochemical growth of metallic nanowires were already described elsewhere [16,17]. Only the most relevant details concerning the electrodeposition of the silver nanowires inside the alumina and polycarbonate templates are described here.

In these experiments, commercially available ANO-PORE<sup>®</sup> porous anodic aluminum oxide (alumina, AAO) membranes purchased from Whatman Company were used, with a thickness of 60  $\mu\text{m}$  and nominal pore diameters of 20 nm. These membranes have two well defined faces: an active one (branched side) formed by interconnected channels with a nominal diameter of 20 nm (corresponding to the pore size claimed by the company) and a thickness of approximately 2  $\mu\text{m}$ . The other face consists of an alumina support layer, formed by unconnected cylindrical pores of 180 nm mean diameter, with a pore density of  $1 \times 10^9$  pores  $\text{cm}^{-2}$  and a thickness of ca. 58  $\mu\text{m}$ . The support layer was used as a template and as a cathode for the nanowire growth, so we will refer in the rest of this article to this effective pore diameter,  $d_p$ . Nanowires were also grown into the pores of commercially available track etched PC (Whatman<sup>®</sup>, Nuclepore Track-Etch Membrane) with nominal pore diameters of 15, 30 and 80 nm specified by the manufacturer (thereafter referred to as  $d_p$ ), with a pore density of  $8 \times 10^8$  per  $\text{cm}^2$  and thickness of 6  $\mu\text{m}$ .

A thin 1500  $\text{\AA}$  gold film was sputtered onto the branched side of the alumina templates and onto one side of the polycarbonate ones. After this, in the case of the alumina templates, the gold film was reinforced with a 20  $\mu\text{m}$  silver film deposited galvanostatically ( $10 \text{ mA cm}^{-2}$ ) from a 0.05 M  $\text{Ag}_2\text{SO}_4 + 2.3 \text{ M KSCN}$  solution.

Electroplating of the nanowires was done in a cylindrical polymethyl methacrylate (PMMA) cell, with the substrate (membrane) facing upward against a hole on the bottom of the cell. A conical carbon counter electrode, facing up the membrane electrode, and an Ag/AgCl (3 M NaCl) reference electrode were used. The nanowire formation was carried out potentiostatically at different overpotential values (the overpotential ( $\eta$ ) is defined as  $\eta = E(I) - E_0$  where  $E(I)$  and  $E_0$  are the applied potential and the equilibrium potential of the electrode, respectively), from a 0.05 M  $\text{Ag}_2\text{SO}_4 + 2.3 \text{ M KSCN}$  solution, pH = 6.0–6.5, without agitation and at room temperature. All the electrochemical experiments were performed with an AUTOLAB PGSTAT 12 potentiostat. The nanowire electrodeposition was monitored by recording current vs. time curves. The deposition process was stopped during growth in the pores, before the formation of caps on top of the wires [16].

Structural characterization of the silver nanowires embedded in alumina and PC membranes was examined by X-ray diffraction (XRD), after mechanically polishing away the back silver film. These spectra were recorded with a Philips PW3710 diffractometer using  $\text{CuK}_\alpha$  radiation. Chemical composition of the silver nanowire array samples were obtained by energy dispersive X-ray analysis (EDS) and was done with the use of a THERMO NORAND VANTAGE (with a NORVARD window)-JEOL 5900 LV SEM equipment. Transmission electron microscopy (TEM) and selected area electron diffraction (SAED) were employed to characterize the individual copper nanowires. These studies were carried out with a Philips CM-200 microscope operated at 200 kV. Details of specimens preparation for TEM are described elsewhere [16,17].

## 3. Results and discussion

Typical X-ray diffractograms for silver nanowire arrays that were grown at an  $\eta = -250 \text{ mV}$ , embedded in polycarbonate ( $d_p = 15 \text{ nm}$ ) and alumina ( $d_p = 180 \text{ nm}$ ) templates, are shown in Figs. 1(a) and (b), respectively. All the diffraction peaks can be indexed as face-centered cubic silver with peak positions which agree very well with those of Ag JCPDS 04-0783 [19], (see Fig. 1(c)), indicating that the face-centered-cubic (fcc) structure of the Ag is preserved in these nanowires.

In the case of the silver nanowire arrays in the 15 nm PC template, X-ray data shows a polycrystalline structure, with a weak (111) preferred orientation. Secondary peaks are (200) and (220). This same crystallographic orientation was also observed in the silver nanowires grown in the different pore size PC membranes under study ( $d_p = 30$  and 80 nm) and at the different overpotentials studied here. In the Ag nanowires embedded in the alumina template a polycrystalline character is also visible. However, the diffraction peak at  $2\theta = 64.4^\circ$  corresponding to the (220) silver plane, is higher than expected for a random polycrystalline sample (see JCPDS pattern), indicating a strong crystallographic orientation: the Ag nanowires have well-preferred orientation along the [220] direction. A very strong [220] preferred crystallographic orientation has also been reported in the literature for silver nanowires electrochemically grown onto alumina templates by cyclic voltammetry [20] and DC electrodeposition [17,21].

Texture analysis was done in order to quantify these strong preferred crystallographic orientations. The textured coefficients (TCs) of preferred orientation were determined by the Harris formula [22]:

$$\text{TC}(hkl) = \frac{I(hkl)/I_0(hkl)}{N^{-1} \sum I(hkl)/I_0(hkl)},$$

where  $\text{TC}(hkl)$  is the texture coefficient of the  $(hkl)$  plane,  $I(hkl)$  is the measured relative intensity of the  $(hkl)$  plane,  $I_0(hkl)$  is the relative intensity of the corresponding plane given in JCPDS data and  $N$  the reflection number. It is clear from the definition that the deviation of the texture

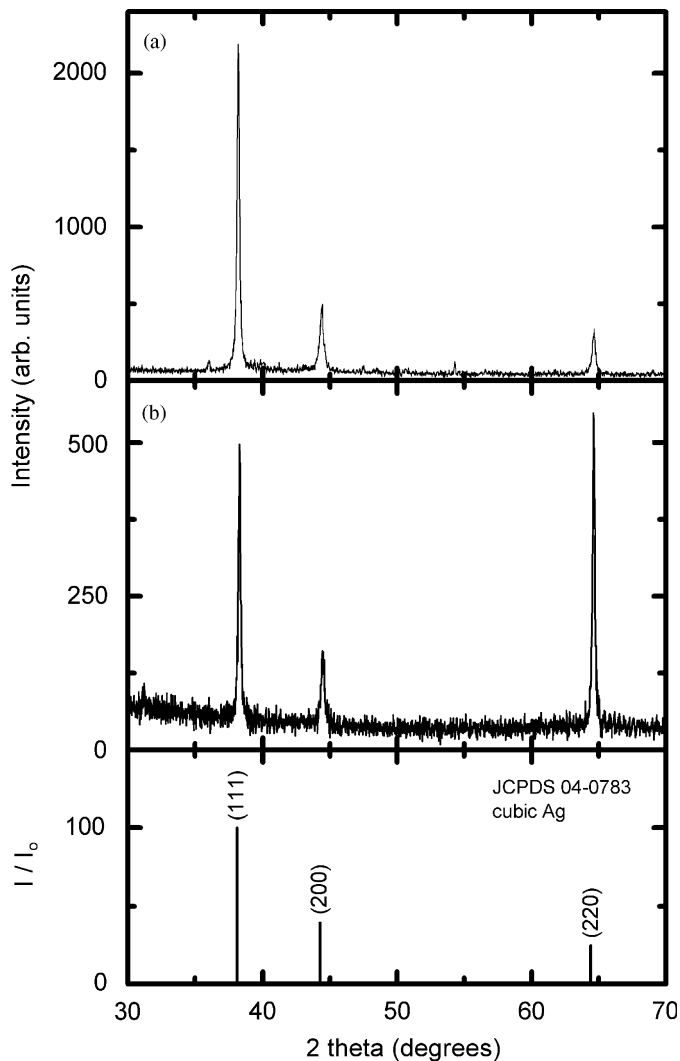


Fig. 1. X-ray diffraction spectrum of the silver nanowire arrays embedded in: (a) polycarbonate template of 15 nm pore size and (b) alumina template of 180 nm pore size.  $\eta = -250$  mV. (c) Ag-JCPDS pattern for comparison.

coefficient from unity implies the preferred orientation of growth of the nanowire. The value of the texture coefficient for the peak in question ranges from unity for a randomly oriented sample to  $N$  for a sample having a complete preferential orientation. The value of the texture coefficient indicates the maximum preferred orientation of the nanowire arrays along the corresponding diffraction plane. Fig. 2 shows the  $TC(111)$  and  $TC(220)$  for the silver nanowire arrays embedded in the 15, 30 and 80 nm polycarbonate and 180 nm AAO templates respectively, as a function of the growth overpotential. It can be seen that the nanowire arrays grown into the PC and AAO templates exhibit a  $TC(111)$  and a  $TC(220)$ , respectively, greater than one. The texture values of the corresponding other reflections are less than one and therefore are not shown in Fig. 2. The arrays of silver nanowires embedded in the PC templates showed a (111) preferred orientation, regardless of pore size. Moreover, it can be seen that the

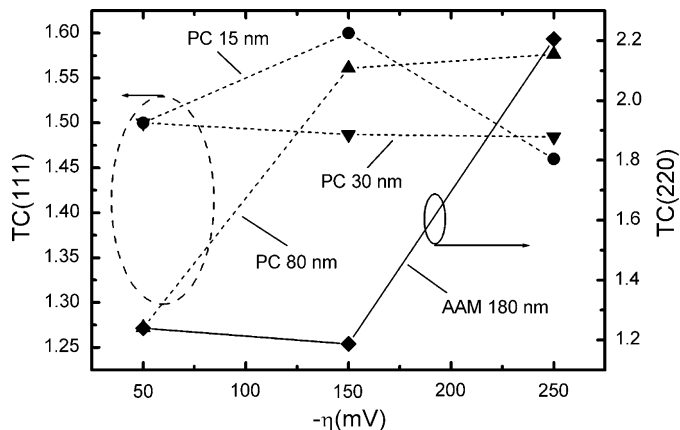


Fig. 2. Variation of  $TC(hkl)$  with deposition overpotential for electrochemically deposited silver nanowire arrays into polycarbonate and alumina templates (pore sizes values as indicated).

nanowires grown inside the biggest pore diameter membranes (i.e.  $d_p = 80$  and 180 nm) showed an increase of their respective texture coefficients with the increase of the overpotential. However, for the same overpotential of  $\eta = -250$  mV, silver nanowires inside the 180 nm AAO template exhibit a degree of texture along the [220] direction which is greater than the correlated [111] inside the 80 nm PC. On the other hand, a texture that appears to be approximately constant or even to decrease somewhat with increasing the overpotential can be seen for nanowires embedded in the 15 and 30 nm pore diameter PC membranes. This difference in texture between the nanowires in PC and those in AAM, must be due to different hydrogen adsorption effects, which may stabilize one plane or the other.

In addition, an XRD study of the influence of template pore diameter on the crystallite size of the silver nanowires was carried out. The dimensions of the crystallites of which the Ag nanowires are composed were estimated from the FWHM of the principal diffraction peaks observed, using the Scherrer formula [23]. When the term “crystallite size” is used, we will be referring to the dimensions of the coherent diffracting domain. This equation is applicable to samples where lattice strain is absent. Nanowires can possess some strains, which could also be a factor contributing to the width of the peaks, thereby affecting estimates of the crystallite size of the nanowires. Moreover, the grain sizes of the silver nanowires estimated from the XRD peak width (and using Scherrer’s formula), were in some cases greater than 90 nm. Thus, grain sizes were larger than the maximum critical values acceptable that can be deduced for these XRD measurements. Therefore, the size of the crystalline domains determined from the XRD peak widths will be used only as a comparative measure among samples. As is shown in Fig. 3, the dimensions of the silver crystallites show an interesting dependence on template pore diameter. Crystallite size increases with increasing pore diameter for  $\eta = -50$  and  $-250$  mV; and

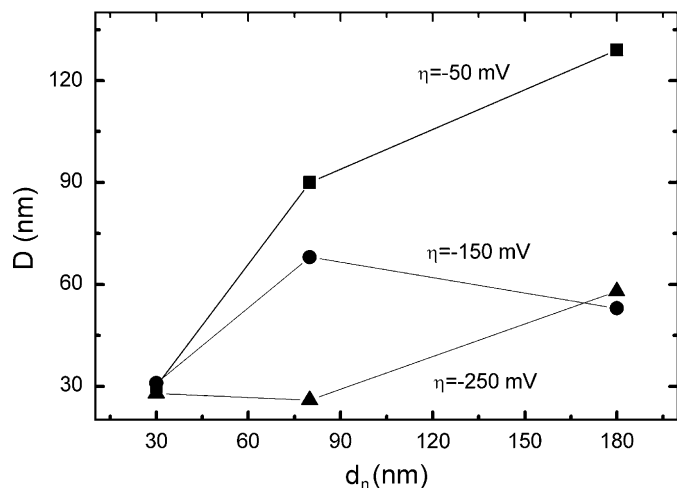


Fig. 3. Average crystallite size of silver nanowire arrays as a function of template pore diameter at different  $\eta$  values as indicated. (30 and 80 nm pore size values correspond to PC membranes, while the 180 nm pore size to an AAO one).

increases up to  $d_p = 80$  nm and afterwards the crystallite dimension seems to be approximately constant or even to decrease for  $\eta = -150$  mV. Hence, it can be deduced that not only is the dimension of the nanowires defined by the pore size of the nanotemplates, but the crystallite size is also correlated. It can also be seen that with low overpotentials bigger crystallites sizes are obtained.

The morphology and the single-crystalline structure of individual nanowires were subsequently investigated by TEM after dissolution of the template. Fig. 4 shows the TEM images of freestanding silver nanowires that have been grown into the 180 nm AAO, 80 and 30 nm PC templates. The TEM observations show that the silver nanowires with a high aspect ratio are dense and continuous. The nanowires grown into the 180 nm AAO and 30 nm PC templates have a uniform diameter of 180 and 60 nm, respectively. However, silver nanowires electrodeposited into the 80 nm PC template have a cigar-like shape, with the same diameter as the nominal value in the end regions, but with a diameter of nearly 160 nm in the central part of each wire. Nickel nanowires with this cigar-like shape, electrodeposited into polycarbonate track-etched membranes, were reported nine years ago by Schönenberger et al. [24]. This shape was attributed to a non-cylindrical shape of the nanoporous inherent to the nuclear track formation process. The insets in Fig. 4 are the corresponding SAED patterns, which indicate that the silver nanowires are high-quality single crystals. An elemental composition analysis of the silver nanowires performed by EDS, revealed (as was expected), that the nanowires consist exclusively of silver atoms. Fig. 4(d) shows a typical EDS spectrum recorded on the silver nanowire arrays, and these peaks only correspond to silver. Moreover, the EDS spectrum does not show indications of any oxide coverage or incorporation.

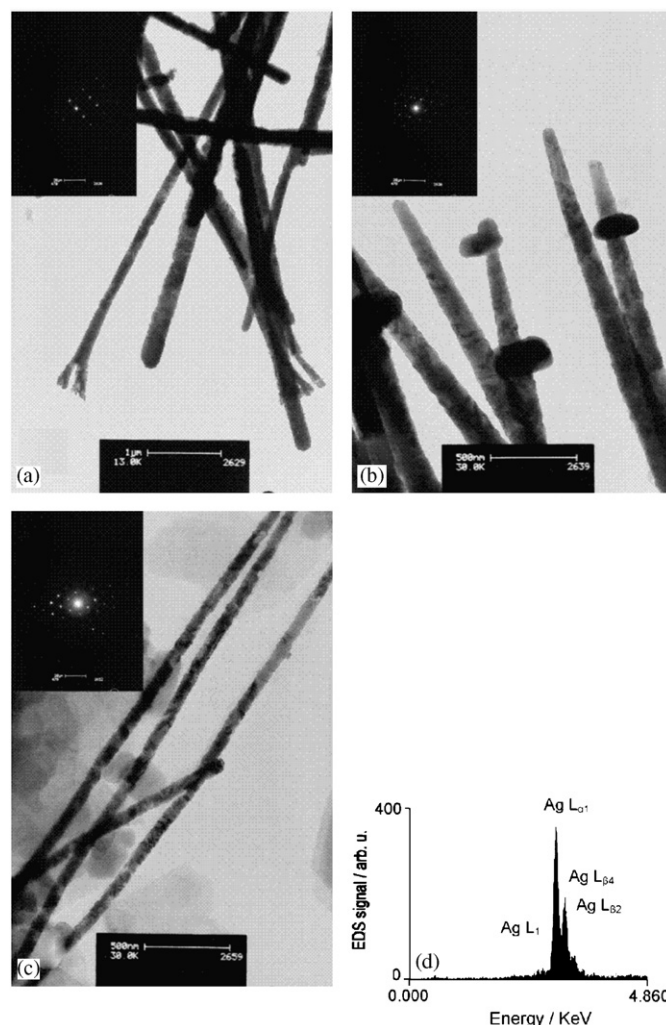


Fig. 4. TEM micrographs of Ag silver nanowires that have been grown at  $\eta = -250$  mV, inside: (a) 180 nm AAO; (b) 80 nm PC and (c) 30 nm PC templates. The insets show the corresponding SAED patterns. (d) EDS elemental analysis of the nanowires, indicating that the only metal element present is silver.  $L_1$ ,  $L_{2,1}$ ,  $L_{\beta 4}$  and  $L_{\beta 2}$  are the transitions responsible for the X-ray fluorescence lines of silver.

#### 4. Conclusions

Silver nanowire arrays were successfully prepared in the pores of AAO and track-etched PC membranes by using the potentiostatic DC electrodeposition technique. Nanowires embedded in the AAO template exhibited a preferred crystallographic orientation along the [220] direction, while those in the PC template exhibited a [111] orientation. In both cases the corresponding textures are enhanced as the overpotential is increased. The crystallite size of the silver nanowires increases as the pore diameter of the templates increases and as the overpotential decreases. Straight, continuous, dense silver nanowires have been obtained, with diameters which ranged from 60 to 180 nm. In general they are uniform in diameter, but those grown in the 80 nm PC template have a cigar-like shape.

## Acknowledgements

E.A.D. carried out this work with the support of the Universidad de Málaga and CSIC (Universidad de la República, Uruguay) which are kindly acknowledged. R.E.M. and E.A.D. thank to CSIC (Universidad de la República), and to PEDECIBA-FISICA, Uruguay. The work has been supported by Junta de Andalucía, Grant FQM0192, CICYT (Spain) Grant TE2004-0051 and Proyecto Fondecyt (Chile) N.: 1040650. The authors also thank to A. Martínez Orellana (Málaga, Spain) for the TEM measurements.

## References

- [1] R.J. Walsh, G. Chumanov, *Appl. Spectrosc.* 55 (2001) 1695.
- [2] A.I. Yanson, G.R. Bollinger, H.E. van den Brom, N. Agrait, J.M. van Ruitenbeek, *Nature* 395 (1998) 783.
- [3] J. Malicka, I. Gryczynski, J. Kusba, Y.B. Shen, J.R. Lakowicz, *Biochem. Biophys. Res. Commun.* 294 (2002) 886.
- [4] D.H. Reich, M. Tanase, A. Hultgren, L.A. Bauer, C.S. Chen, G.J. Meyer, *J. Appl. Phys.* 93 (2003) 7275.
- [5] G. Yi, W. Schwarzacher, *Appl. Phys. Lett.* 74 (1999) 1746.
- [6] M. Tian, J. Wang, J. Snyder, J. Kurtz, Y. Liu, P. Schiffer, T.E. Mallouk, M.H. Chan, *Appl. Phys. Lett.* 83 (2003) 1620.
- [7] K. Liu, C.L. Chien, P.C. Searson, K. Yu-Zhang, *Appl. Phys. Lett.* 73 (1998) 1436.
- [8] J. Heremans, C.M. Thrush, Y.-M. Ling, S. Cronin, Z. Zhang, M.S. Dresselhaus, J.F. Mansfield, *Phys. Rev. B* 61 (2000) 2921.
- [9] Y.-G. Guo, L.-J. Wan, C.-F. Zhu, D.-L. Yang, D.-M. Chen, C.-L. Bai, *Chem. Mater.* 15 (2003) 664.
- [10] D.N. Davydov, P.A. Sattari, D. Almalawi, A. Osika, T.L. Haslett, M. Moskovits, *J. Appl. Phys.* 86 (1999) 3983.
- [11] M. Martín-González, A.L. Prieto, M.S. Kox, R. Gronsky, T. Sands, A.M. Stacy, *Chem. Mater.* 15 (2003) 1676.
- [12] D.J. Pena, B. Razavi, P.A. Smith, J.K. Mdingo, M.J. Natan, T.S. Mayer, T.E. Mallouk, C.D. Keating, *Mater. Res. Soc. Symp.* 636 (2001) D.4.6.1.
- [13] G.E. Possin, *Rev. Sci. Instrum.* 41 (1970) 772.
- [14] C.R. Martin, *Science* 266 (1994) 1961.
- [15] M.S. Dresselhaus, Y.M. Lin, O. Rabin, M.R. Black, G. Dresselhaus, *Nanowires*, in: B. Bhushan (Ed.), *Springer Handbook of Nanotechnology*, Springer, Berlin, 2004, p. 99.
- [16] G. Riveros, H. Gómez, A. Cortes, R.E. Marotti, E.A. Dalchiele, *Appl. Phys. A* 81 (2005) 17.
- [17] G. Riveros, S. Green, A. Cortes, H. Gómez, R.E. Marotti, E.A. Dalchiele, *Nanotechnology* 17 (2006) 1.
- [18] Y. Cao, W. Liu, J. Sun, Y. Han, J. Zhang, S. Liu, H. Sun, J. Guo, *Nanotechnology* 17 (2006) 2378.
- [19] JCPDS Silver, File 04-0783.
- [20] X.-Y. Sun, F.-Q. Xu, Z.-M. Li, W.-H. Zhang, *Mater. Chem. Phys.* 90 (2005) 69.
- [21] J. Zhang, X. Wang, X. Peng, L. Zhang, *Appl. Phys. A* 75 (2002) 485.
- [22] G.B. Harris, *Philos. Mag.* 43 (1952) 113.
- [23] B.D. Cullity, *Elements of X-ray Diffraction*, second ed., Addison Wesley, Reading, MA, 1978.
- [24] C. Schönenberger, B.M. van der Zande, L.G.J. Fokking, M. Henry, C. Schimid, M. Krüger, A. Bachtold, R. Huber, H. Birk, U. Stauffer, *J. Phys. Chem.* 101 (1997) 5497.